Journal of Industrial and Engineering Chemistry 76 (2019) 240–244

Contents lists available at ScienceDirect

Journal of Industrial and Engineering Chemistry

journal homepage: www.elsevier.com/locate/jiec

# Adsorption of metal ions with biochars derived from biomass wastes in a fixed column: Adsorption isotherm and process simulation

Yu Ping Zhang[a], Vincentius Surya Kurnia Adi[b], Hsin-Liang Huang[a,*], Hong-Ping Lin[c], Zi-Hao Huang[a]

[a] Department of Safety, Health and Environmental Engineering, National United University, Miaoli 36063, Taiwan
[b] Department of Chemical Engineering, National Chung Hsing University, Taichung 402, Taiwan
[c] Department of Chemistry, National Cheng Kung University, Tainan City 701, Taiwan

ARTICLE INFO

*Article history:*
Received 20 March 2018
Received in revised form 2 March 2019
Accepted 27 March 2019
Available online 4 April 2019

*Keywords:*
Biochar
Biomass waste
Competitive metal adsorption
Process simulation

ABSTRACT

Biochars were derived from wood and water caltrop shell waste for the adsorption of Cr(III) and Cu(II) in solutions. In the competitive adsorption, Cu(II) had a good affinity for the water caltrop shell and blended biochars. The blended biochar was a mixture of wood and water caltrop shell biochars. Each biochar adsorption equilibrium data fit well with the Freundlich model. The effectiveness of the adsorption of Cr (III) and Cu(II) solutions utilizing biochar is proven to be effective in continuous adsorption columns, and the adsorption performance is verified with model simulation.


## Introduction

The wastewaters, which contain metals, are discharged from industrial processes and need to be treated using several steps due to the low pH and content of one or more metal ions. Copper (Cu) and chromium (Cr) compounds are used in mining, plating and petroleum industries and are also emitted into wastewaters [1–4]. Cu compounds are suspected of being carcinogenic and could cause breast or lung cancer [5,6]. Although trivalent Cr (Cr (III)) has less toxicity than hexavalent Cr (Cr(VI)), the concentration of Cr(III) in the wastewater is still limited by effluent standards [7,8]. The methods for metal removal from wastewaters are adsorption, precipitation, ion exchange, coagulation, and electrodialysis [9–13]. Adsorption is an economical method and is applied for treatment for low concentrations of metal from large volumes of wastewater [14,15]. Moreover, the adsorption efficiency is high in removing metals from solutions.

Porous carbon and silica, metal-based adsorbents, bioadsorbents, clay, and sewage sludge, are used as adsorbents to remove metal ions from wastewaters [16–21]. Biochars, which are stable, carbon-rich and porous materials, are produced from biomass under oxygen-limited conduction in the thermal process [22,23]. In Taiwan, five to six million tons of agricultural and forestry wastes are discarded every year. The wastes are usually dealt with by incineration, which leads to the release of large amounts of carbon dioxide into the atmosphere. Low-cost biochar can be derived from the biomass wastes for recycling. The properties of biochar are the high surface area, porosity, neutral to alkaline pH and functional groups [22]. Therefore, original and modified biochars are used as sorbents for remediation of organic and inorganic pollutants [24,25]. Arsenic, cadmium, chromium, copper, lead, and zinc can be adsorbed on biochars produced from hardwood, oak wood or crop straw [26–30]. After the activation of biochar, the high adsorbed concentration of Cu(II) on biochar occurs [31]. The adsorption efficiencies of Cr(VI) and Pb(II) are dependent on the pH of the biochars with a high surface area and functional groups [32]. The adsorption efficiencies of metal ions in water are influenced by biochar properties. In the competitive adsorptions, it was evident that the efficiency of Cr(III) was affected by the surface area of the biochar more than Cu(II) [33,34].

Moreover, the adsorption efficiency was affected by the nature of the metals in competitive adsorptions. The adsorption capacities on biochar significantly changed between monometal and multi-metal adsorption conductions [35]. The concentration of Cd(II) on engineered biochar is higher than As(V). However, Ni(II) has a stronger affinity for engineered biochar than Cd(II) [36]. The competitive adsorptions of metals by signal and blended biochars are seen as limited in the literatures.

In this study, two biochars were prepared from wood and water caltrop shell wastes. The adsorbed capacities of biochars for Cr(III)

* Corresponding author.
*E-mail address:* hlhuang@nuu.edu.tw (H.-L. Huang).

https://doi.org/10.1016/j.jiec.2019.03.046
1226-086X/

and Cu(II) in the solutions were investigated by bath experiments. In the previous literature, blended biochar performance has not been addressed significantly. Therefore, this study tries to evaluate how blended biochar performs as a proof of concept in comparison with single biochar ones. The adsorption isotherm of single and blended biochars for Cr(III) and Cu(II) were evaluated in competitive adsorptions.

Furthermore, the adsorption operation of metals from water is mostly in a continuous mode [37]. The fixed-bed column study can be implemented to describe the dynamic interaction of the adsorption process. Hence, a lab-scale model of the adsorption tower was also built to verify the simulation results and reciprocally provided parameter data for process simulation.

## Methods and materials

### *Preparation of biochars*

Wood and water caltrop shell wastes were collected from farmland in southern Taiwan. Pyrolysis of wood and water caltrop shell wastes were conducted at around 1073–1173 K under oxygen-limited conduction for 0.5–1.0 h, respectively. After washing with $H_2O$, the wood and water caltrop shell biochars were dried at 343 K to remove the $H_2O$. The particle sizes of the wood and water shell biochars were individualized by screening in the range of 0.02–0.043 mm, respectively. The blended biochar was composed of mixed wood and water caltrop shell biochars at the weight ratio of 1:1. The surface areas and pore sizes of the biochars were measured with a specific surface area and pore size distribution analyzer using the Gas adsorption method (Micromeritics ASAP 2020). Table 1 shows the properties of each biochar.

### *Effect of initial solution pH*

A 750 ppm of Cr(III) solution was prepared by dissolving 0.96 g $CrCl_3{\cdot}6H_2O$ (93%, Showa) in deionized water and poured into 250 mL volumetric flask, then add deionized water to the marking line at 298 K. The 20 mL Cr(III) solutions with different pH levels were mixed individually with 0.03 g of each biochar at 298 K for four hours. The preparation of 750 ppm Cu(II) solution and adsorption of Cu(II) on each biochar were also processed in similar ways. $Cu(NO_3)_2{\cdot}3H_2O$ (99%, Showa) was used as the Cu(II) species. The pH solutions were adjusted to 2, 3 and 4 by 1M $HNO_3$ (69.0–70.0%, J.T. Baker) and 1M NaOH (97%, Showa).

### *Adsorption isotherms*

A solution of 500 ppm Cr(III) and 500 ppm Cu(II) was prepared by dissolving 0.64 g $CrCl_3{\cdot}6H_2O$ and 0.48 g $Cu(NO_3)_2{\cdot}3H_2O$ in deionized water and poured into 250 mL volumetric flask, then add deionized water to the marking line at 298 K. The solution which contained 500 ppm Cr(III) and 500 ppm Cu(II) was diluted to concentrations at 25, 50 and 250 ppm for each metal. 20 mL of the different concentration solutions at pH 2 were mixed with 0.03 g of each biochar at 298 K for four hours. The Freundlich adsorption equation was used to explain the adsorption isotherms:

$$q_e = K_f C_e^{1/n}$$

where $q_e$ (mg/g) is the equilibrium concentration of the adsorbed metal in the biochar, $Ce$ (mg/L) is the equilibrium concentration of metal in the solution and $K_f$ and $n$ are the constants associated with the adsorption capacity ((mg/g)(L/mg)$^{1/n}$) and intensity of the adsorption, respectively.

### *Fixed bed adsorption column*

Fixed bed column experiments were conducted in a glass column with a 1 cm inner diameter and a 6–7 cm height. Approximately 2.2–2.5 g of blended biochar were packed into the column. The Cr(III) and Cu(II) solution was introduced at 1 mL/min into the column using a peristaltic pump (EYELA, MP-2000) at 298 K. Aspen Adsorption® V10.0 was utilized as a comprehensive flowsheet simulator for the optimal design, simulation, optimization and analysis of the adsorption processes. A parameter estimation to determine the dispersion coefficient of the packed column system was implemented to fit the models against experimental and simulated data.

### *Instrumental techniques*

An Atomic absorption spectrometer (Hitachi ZA3300) was applied to determine the concentrations of Cr and Cu in triplicate in the solution after the adsorption processes. The Cr and Cu concentrations of the calibration curves were 0.1–10.0 ppm with the correlation coefficient >0.9995. The functional groups of biochars before and after adsorption were recorded on a Fourier transform infrared (FTIR) spectrometer (Nicolet 6700). For all spectra reported, a 128-scan data accumulation was conducted at a resolution of 4 $cm^{-1}$.

## Results and discussion

### *The effect of solution pH*

The species of Cr(III) is $Cr^{3+}$ at pH <3.6 [23]. At pH 3.6–5, $Cr^{3+}$ and $Cr(OH)^{2+}$ are the main species [38]. Therefore, the pH levels of the solutions were adjusted to 2, 3 and 4 in order to maintain the desired chromium species in the adsorption processes. Table 2 shows that the maximum adsorption capacities of wood and water caltrop shell biochars for Cr(III) were 67.7 and 78.5 mg/g at pH 2, respectively. The surface area of biochars affects adsorption capacity. Therefore, the adsorption capacity of water caltrop shell biochar for Cr(III) was higher than that of wood biochar at pH levels of 2, 3 and 4. The capacity of wood biochar for Cu(II) is also a maximum at pH 2. However, the Cu(II) solution with pH 3 can adsorb effectively on the water caltrop shell biochar. The pH levels of the solutions were adjusted to 2 in order to obtain the highest amounts of Cr(III), and Cu (II) absorbed on wood and water caltrop shell biochars.

**Table 1**
Properties of wood, water caltrop shell and blended biochars.

| | Wood biochar | Water caltrop shell biochar | Blended biochar |
|---|---|---|---|
| pH | 9.8 | 9.94 | 9.77 |
| Surface area ($m^2$/g) | 198 | 264 | 225 |
| Pore size (nm) | < 2.0 | < 2.0 | < 2.0 |
| Cation exchange capacity (meq/100 g) | 18.2 | 18.8 | Not measured |

**Table 2**
Effects of pH on the concentration of single metal adsorption on biochars.

| | | Adsorption capacity (mg/g) | |
|---|---|---|---|
| | pH | Wood biochar | Water caltrop shell biochar |
| Cr(III) | 2 | 67.7 | 78.5 |
| | 3 | 45.5 | 62.3 |
| | 4 | 57.6 | 68.4 |
| Cu(II) | 2 | 49.8 | 48.5 |
| | 3 | 48.6 | 51.6 |
| | 4 | 34.0 | 45.8 |

*FTIR spectroscopy*

Fig. 1(a) and (d) shows the functional groups of wood and water caltrop shell biochar before and after in acidic solutions ($HNO_3$) at pH 2, 3, and 4, respectively. A peak at 1566 $cm^{-1}$ for wood biochar corresponding to C=C stretching was observed barely just after in the acidic solution and adsorption of Cr(III) and Cu(II) at pH 2, 3 and 4 (see Fig. 1(a)–(c)) [39]. The redshift of the feature at 1440 $cm^{-1}$ for wood biochar is related to its stretching of –COO– to 1384.6 $cm^{-1}$ and is seen as an interaction between $H^+$ and the wood biochars in the acidic solution at pH 2 (see Fig. 1(a)). In Fig. 1(b) and (c), it is also found that interactions between metal ions (Cr(III) and Cu(II)) and the wood biochars were significant at 1384.6 $cm^{-1}$ after adsorption [40]. Moreover, the aromatic –CH stretching at 873 $cm^{-1}$ shows a redshift to 838.7 $cm^{-1}$ in Fig. 1(c) [40]. In the water caltrop shell biochar, the shifts of peaks of C=C and —CH stretching (at 1566 and 873 $cm^{-1}$, respectively) were also observed just after in acidic solutions and adsorption of metal ions (see Fig. 1(d)–(f)). The water caltrop biochar had a –COO– stretching similar to the wood biochar (at 1434 $cm^{-1}$) (see Fig. 1(d)). The redshift (1434 → 1384.6 $cm^{-1}$) for the –COO– stretching associated with $H^+$ was also found. The similar results on significant interactions between Cr(III) and Cu(II) species and –COO– were also observed (see Fig. 1(e) and (f)). The concentrations of adsorbed Cr(III) and Cu(II) were mainly affected by –COO– of biochars.

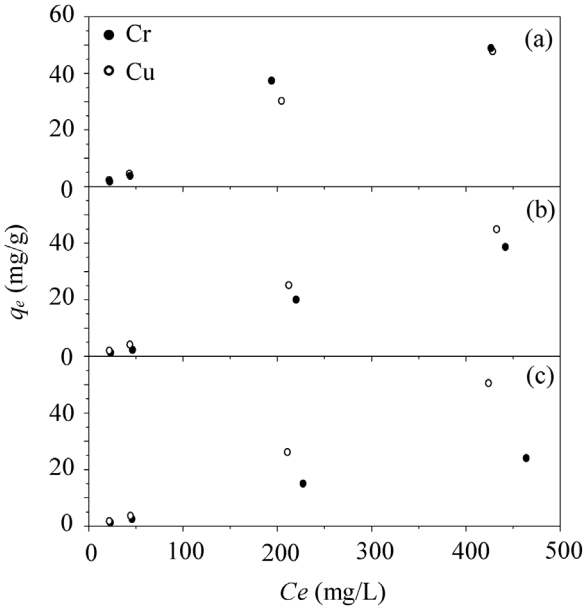


**Fig. 2.** Adsorption isotherm of metals on (a) wood biochar, (b) water caltrop shell biochar and (c) blended biochar (wood biochar: water caltrop shell biochar = 1:1 (wt)).

*Adsorption isotherms*

In Fig. 2, the adsorbed concentrations of metal ions (Cr(III) and Cu(II)) on biochars were raised with an increase in *Ce*. Fig. 2(a) shows that the adsorbed concentration of Cr(III) on the wood biochar was a little higher than that of Cu(II) in the competitive adsorption. However, the adsorbed concentration of Cu(II) on water caltrop shell biochar was 1.2–1.7 times higher than that of Cr(III) (see Fig. 2(b)). Furthermore, the Cu(II) was the main adsorbed species on the blended biochar in Fig. 2(c). The concentration of Cu(II) was observed to be 1.38–2.11 times more than that of Cr(III) on the blended biochar. The results are different from the concentration of single metal adsorption on biochars (see Table 2). The electronegativities of Cu(II) and Cr(III) were 1.90 and 1.66, respectively [41].

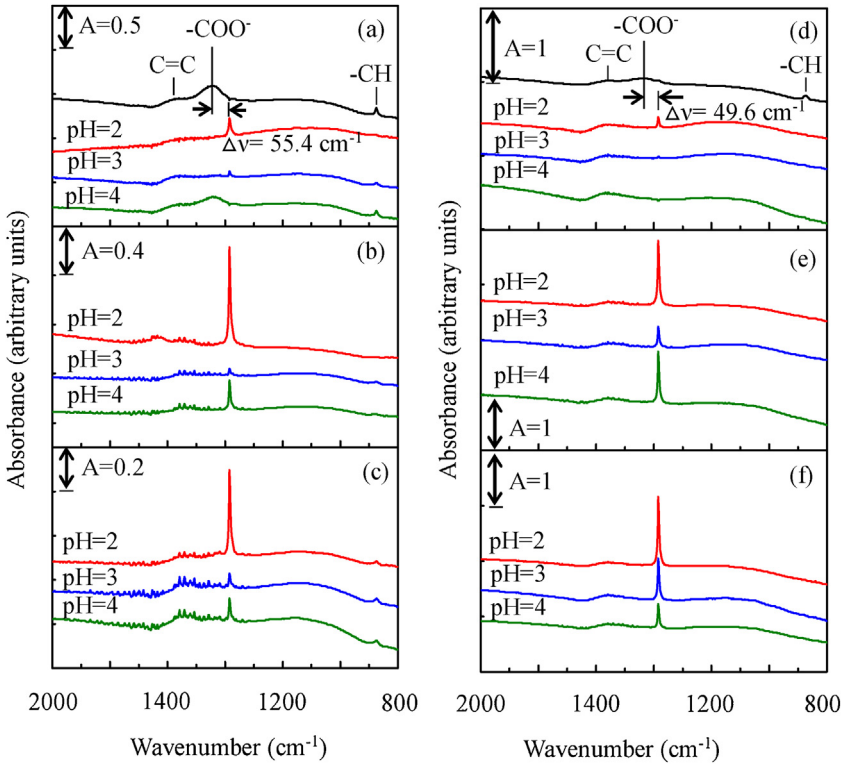


**Fig. 1.** Infrared spectra of (a) original, (b) Cr-adsorbed and (c) Cu-adsorbed wood biochar at different pH and the (d) original, (e) Cr-adsorbed and (f) Cu-adsorbed water caltrop shell biochar at different pH by FTIR spectroscopy.

**Table 3**
Freundlich isotherm parameters for Cr(III) and Cu(II) adsorption on biochars.

| | | Freundlich model | | |
|---|---|---|---|---|
| | | $K_f$ ((mg/g)(L/mg)$^{1/n}$) | $1/n$ | $R^2$ |
| Wood biochar | Cr | 0.040 | 1.22 | 0.969 |
| | Cu | 0.083 | 1.07 | 0.991 |
| Water caltrop shell biochar | Cr | 0.024 | 1.23 | 0.995 |
| | Cu | 0.073 | 1.07 | 0.997 |
| Blended biochar | Cr | 0.057 | 1 | 0.995 |
| | Cu | 0.048 | 1.15 | 0.998 |

$R^2$: correlation coefficient.

Therefore, Cu(II) had a good affinity for the water caltrop shell and blended biochars in the competitive adsorption.

The Freundlich isotherm model provided the Freundlich adsorption equation used to fit the adsorption data for metal ions (Cr(III) and Cu(II)) on wood, water caltrop shell and blended biochars. Table 3 shows the estimated parameters of the Freundlich isotherm. The correlation coefficients ($R^2$) for Cr(III) and Cu(II) adsorbed on wood, water caltrop shell, and blended biochars were 0.969–0.998. Therefore, the Freundlich isotherm shows the best fit for the experimental data. The Freundlich isotherm constant n for Cr(III) adsorbed on blended biochar was one, which indicates linear adsorption.

*Process simulation*

According to the Freundlich isotherm obtained from the previous experiment, a continuous adsorption column was developed accordingly for blended biochars system in Aspen Adsorption® V10.0 (see Fig. 3). The liquid adsorption process is chosen to represent the mechanism of the current system. The biochars bed model assumes:

- plug flow with axial dispersion where the dispersion coefficient is constant for all components throughout the bed,
- The liquid phase pressure is constant,
- The superficial velocity is constant, so adsorption from the liquid phase has a negligible effect on the material balance. These assumptions are valid as the system corresponds to the removal of trace components from a bulk liquid.
- Molar concentrations are calculated from molar volumes. Ideal mixing is assumed to occur in the liquid phase, so molar volume is a linear function of composition,
- A lumped mass-transfer rate applies, with a solid-film linear resistance,
- Mass transfer coefficients are assumed to be constant,
- The adsorption isotherm is chosen to be Freundlich model with independent temperature following the estimated parameter values shown in Table 3,
- Isothermal conditions apply.

The simulation is carried out for the blended biochars system in particular since it is deemed as the potential alternative in this study. The outlet concentration profile for Cr(III) and Cu(II) from the lab scale adsorption tower is provided in Figs. 4 and 5. The adsorption performance of biochars can be observed where both Cr(III) and Cu(II) were treated entirely in the first 2500 s of operation for a 500 ppm inlet concentration. With a lower inlet concentration of 250 ppm, the adsorption breakthrough curve was found to be longer at around 3500 s. The corresponding breakthrough curves from the simulation are quite similar to that of the experimental data, which indicates that the adsorption parameters obtained from the previous experiments are valid (see Figs. 4 and 5). From the breakthrough curves of the experimental data, it can be concluded that dispersion plays a significant role in the current column system. By utilizing the

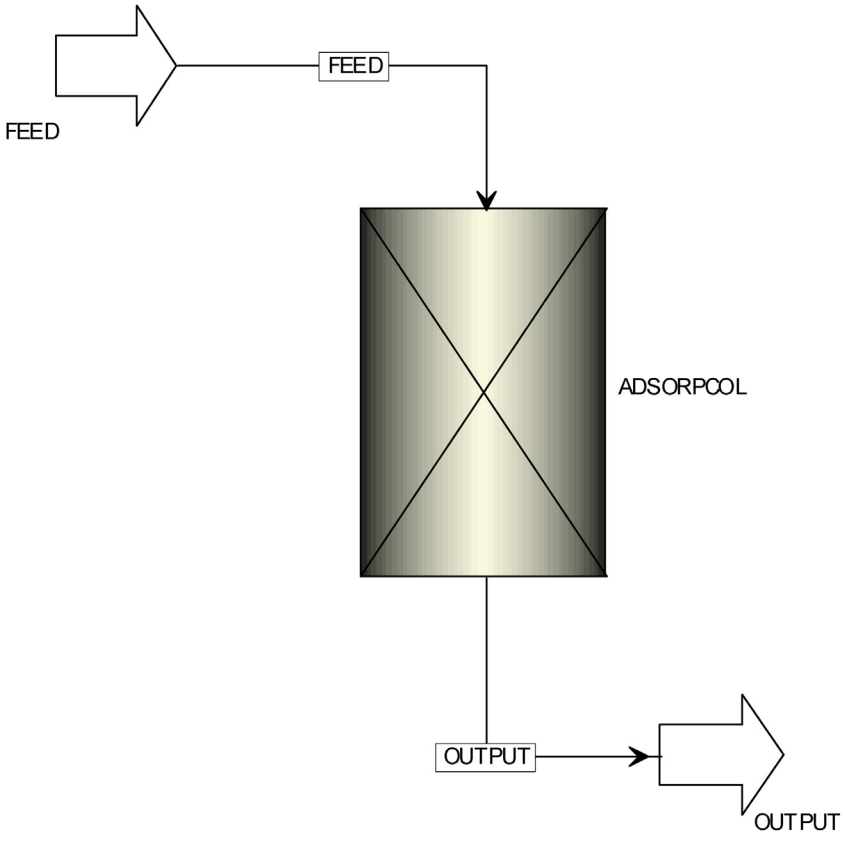


**Fig. 3.** Aspen adsorption flowsheet model.

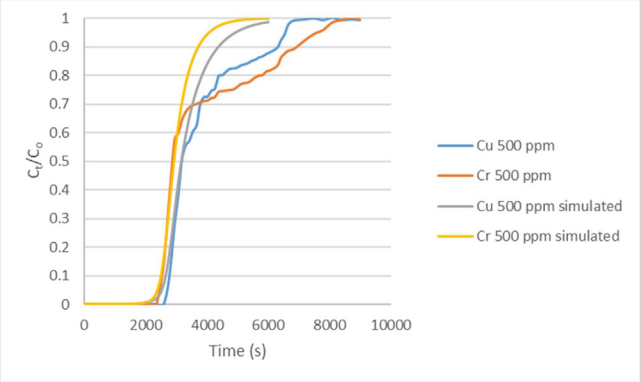


**Fig. 4.** Breakthrough curve for 500 ppm inlet concentration.

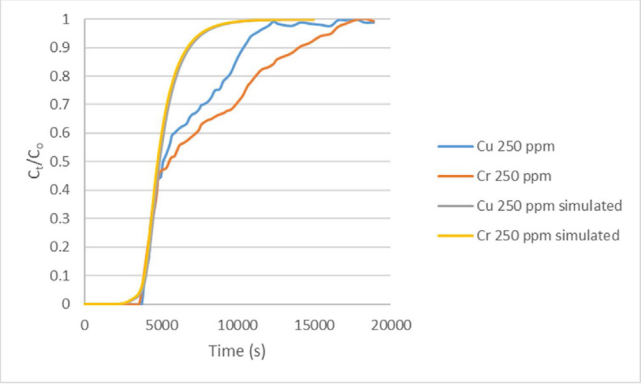


**Fig. 5.** Breakthrough curve for 250 ppm inlet concentration.

built-in parameter estimation of Adsorption® V10.0, the dispersion coefficient of the column system is found to be $2 \times 10^{-6}\,m^2\,s^{-1} \pm 10\%$. Although there are unexplained nonidealities at later times, the simulation model can be considered to be representative for the current case study.

## Conclusions

The adsorption capacities of wood and water caltrop shell biochars for Cr(III) were higher than those for Cu(II) in single metal adsorption. Using FTIR spectroscopy, the adsorbed concentrations of Cr(III) and Cu(II) were mainly affected by −COO− on wood and water caltrop shell biochars. In competitive adsorption, a good affinity for Cu(II) on water caltrop shell and blended biochars was obtained. All adsorption isotherm data can be fitted by the Freundlich model. The simulation results were verified with the experimental data, and the performance of the biochar adsorption column can be predicted quite accurately with the available parameters from previous experiments. Moreover, the simulation results show the feasibility of utilizing blended biochar in an adsorption column setting.

## Acknowledgments

The financial supports of National United University (107-NUUPRJ-04) and Taiwan Ministry of Science and Technology (MOST 106-2221-E-005-095) are gratefully acknowledged.

## References

[1] B. Prasad, J.M. Bose, Environ. Geol. 41 (2001) 183.
[2] C.G. Lee, S. Lee, J.A. Park, C. Park, S.J. Lee, S.B. Kim, B. An, S.T. Yun, S.H. Lee, J.W. Choi, Chemosphere 166 (2017) 203.
[3] M.D. Machado, E.V. Soares, H.M.V.M. Soares, Environ. Sci. Pollut. Res. 18 (2011) 1279.
[4] J.W. Patterson, Waste Water Treatment, Science Publishers, New York, 1997.
[5] M. Kucharzewski, J. Braziewicz, U. Majewska, S. Gozdz, Biol. Trace Elem. Res. 93 (2013) 9.
[6] F. Dehdashti, M.A. Mintun, J.S. Lewis, J. Bradley, R. Govindan, R. Laforest, M.J. Welch, B.A. Siegel, Eur. J. Nucl. Med. Mol. Imaging 30 (2003) 844.
[7] Environmental Protection Administration, Effluent standards in water pollution control Taiwan, (2011) .
[8] Ministry of the Environment, National effluent standards in water quality Japan, (2015) .
[9] M. Renu, K. Agarwal, Singh, J. Water Reuse Desalin. 7 (2017) 387.
[10] N.K. Srivastava, C.B. Majumder, J. Hazard. Mater. 151 (2008) 1.
[11] S.A. Cavaco, S. Fernandes, M.M. Quina, L.M. Ferreira, J. Hazard. Mater. 144 (2007) 634.
[12] F.L. Fu, Q. Wang, J. Environ. Manage. 92 (2011) 407.
[13] S.J. Ye, G.M. Zeng, H.P. Wu, C. Zhang, J. Dai, J. Liang, J.F. Yu, X.Y. Ren, H. Yi, Cheng M, Crit. Rev. Biotechnol. 37 (2017) 1062.
[14] D. Sud, G. Mahajan, M.P. Kaur, Bioresour. Technol. 99 (2008) 6017.
[15] H.A.M. Bacelo, S.C.R. Santos, C.M.S. Botelho, Chem. Eng. J. 303 (2016) 575.
[16] V.V. Kulkarni, A.K. Golder, P.K. Ghosh, J. Hazard. Mater. 341 (2018) 207.
[17] E. Da'na, Microporous Mesoporous Mater. 247 (2017) 145.
[18] A. Goswami, P.K. Raul, M.K. Purkait, Chem. Eng. Res. Des. 90 (2012) 1387.
[19] M. Abdulazizi, S. Musayev, Pol. J. Environ. Stud. 26 (2017) 1433.
[20] Y.S. Al-Degs, M.I. El-Barghouthi, A.A. Issa, M.A. Khraisheh, G.M. Walker, Water Res. 40 (2006) 2645.
[21] F. Rozada, M. Otero, A. Moran, A.I. Garcia, J. Hazard. Mater. 99 (2008) 6332.
[22] M. Ahmad, A.U. Rajapaksha, J.E. Lim, M. Zhang, N. Bolan, D. Mohan, M. Vithanage, S.S. Lee, Y.S. Ok, Chemosphere 99 (2014) 19.
[23] H.B. Li, X.L. Dong, E.B. da Silva, L.M. de Oliveira, Y.S. Chen, L.N.Q. Ma, Environ. Pollut. 178 (2017) 466.
[24] H.P. Wu, C. Lai, G.M. Zeng, J. Liang, J. Chen, J.J. Xu, J. Dai, X.D. Li, J.F. Liu, M. Chen, L.H. Lu, L. Hu, J. Wan, Crit. Rev. Biotechnol. 37 (2017) 754.
[25] Z.T. Zeng, S.J. Ye, H.P. Wu, R. Xiao, G.M. Zeng, J. Liang, C. Zhang, J.F. Yu, Y.L. Fang, B. Song, Sci. Total Environ. 648 (2019) 206.
[26] W. Hartley, N.M. Dickinson, P. Riby, N.W. Lepp, Environ. Pollut. 157 (2009) 2654.
[27] X. Chen, G.C. Chen, L.G. Chen, Y.X. Chen, J. Lehmann, M.B. McBride, A.G. Hay, Bioresour. Technol. 102 (2011) 8877.
[28] D. Mohan, S. Rajput, V.K. Singh, P.H. Steele, C.U. Pittman, J. Hazard. Mater. 188 (2011) 319.
[29] N. Karami, R. Clemente, E. Moreno-Jimenez, N.W. Lepp, L. Beesley, J. Hazard. Mater. 191 (2011) 41.
[30] X.J. Tong, J.Y. Li, J.H. Yuan, R.K. Xu, Chem. Eng. J. 172 (2011) 828.
[31] H.D.S.S. Karunarathne, B.M.W.P.K. Amarasinghe, Eng. Procedia 34 (2013) 83.
[32] W. Zhang, S.Y. Mao, H. Chen, L. Huang, R.L. Qiu, Bioresour. Technol. 147 (2013) 545.
[33] A.G. Caporale, M. Pigna, A. Sommella, P. Conte, Biol. Fertil. Soils 50 (2014) 1211.
[34] S.J. Ye, G.M. Zeng, H.P. Wu, C. Zhang, J. Liang, J. Dai, Z.F. Liu, Xiong W.P, J. Wan, P. A. Xu, M. Cheng, Crit. Rev. Nev. Sci. Technol. 47 (2017) 1528.
[35] J.H. Park, Y.S. Ok, S.H. Kim, J.S. Cho, J.S. Heo, R.D. Delaune, D.C. Seo, Chemosphere 142 (2016) 77.
[36] K. Yoon, D.W. Cho, D.C.W. Tsang, N. Bolan, J. Rinklebe, H. Song, Bioresour. Technol. 246 (2017) 69.
[37] S. Vilvanathan, S. Shanthakumar, Environ. Prog. Sustain. Energy 36 (2017) 1030.
[38] T. Wang, W. Liu, L. Xiong, N. Xu, J. Ni, Chem. Eng. J. 215–216 (2013) 366.
[39] A. Cibati, B. Foereid, A. Bissessur, S. Hapca, J. Clean Prod. 162 (2017) 1285.
[40] P.J. He, Q.F. Yu, H. Zhang, L.M. Shao, F. Lu, Sci. Rep. 7 (7091) (2017).
[41] M.B. McBride, Environmental Chemistry of Soils, Oxford University Press, New York, 1994.